ARTICLE

Bone marrow adipose tissue-derived stem cell factor mediates metabolic regulation of hematopoiesis

Zengdi Zhang,[1*] Zan Huang,[1,2,3*] Brianna Ong,[1] Chinmayi Sahu,[1] Hu Zeng,[4,5] and Hai-Bin Ruan[1,6]

[1]Department of Integrative Biology and Physiology, University of Minnesota Medical School, Minneapolis, MN, USA; [2]Laboratory of Gastrointestinal Microbiology, Jiangsu Key Laboratory of Gastrointestinal Nutrition and Animal Health, College of Animal Science and Technology, Nanjing Agriculture University, Nanjing, Jiangsu, China; [3]National Center for International Research on Animal Gut Nutrition, Nanjing Agriculture University, Nanjing, Jiangsu, China; [4]Division of Rheumatology, Department of Medicine, Mayo Clinic, Rochester, MN, USA; [5]Department of Immunology, Mayo Clinic, Rochester, MN, USA and [6]Center for Immunology, University of Minnesota, Minneapolis, MN, USA

These authors contributed equally.

Ferrata Storti Foundation

Haematologica 2019
Volume 104(9):1731-1743

ABSTRACT

Hematopoiesis is dynamically regulated by metabolic cues in homeostatic and stressed conditions; however, the cellular and molecular mechanisms mediating the metabolic sensing and regulation remain largely obscure. Bone marrow adipose tissue remodels in various metabolic conditions and has been recently proposed as a niche for hematopoietic stem cells after irradiation. Here, we investigated the role of marrow adipose tissue-derived hematopoietic cytokine stem cell factor in unperturbed hematopoiesis by selectively ablating the *Kitl* gene from adipocytes and bone marrow stroma cells using *Adipoq-Cre* and *Osx1-Cre*, respectively. We found that both *Adipoq-Kitl* knockout (KO) and *Osx1-Kitl* KO mice diminished hematopoietic stem and progenitor cells and myeloid progenitors in the bone marrow and developed macrocytic anemia at the steady-state. The composition and differentiation of hematopoietic progenitor cells in the bone marrow dynamically responded to metabolic challenges including high fat diet, β3-adrenergic activation, thermoneutrality, and aging. However, such responses, particularly within the myeloid compartment, were largely impaired in *Adipoq-Kitl* KO mice. Our data demonstrate that marrow adipose tissue provides stem cell factor essentially for hematopoiesis both at the steady state and upon metabolic stresses.

Introduction

The metabolic and hematopoietic systems demonstrate dynamic and complex interplays in health and disease. On the one hand, a plethora of blood cells including granulocytes, monocytes and macrophages, mast cells, and lymphocytes contribute to the physiological and pathological regulation of energy intake and expenditure, glucose and lipid metabolism, bone remodeling, and the aging process.[1-4] On the other hand, hematopoietic stem cells (HSC), myeloid and lymphoid progenitors, and their mature progeny not only impose different bioenergetic demands during development,[5-8] but also show flexibility and plasticity in their maintenance, differentiation, and function in response to various metabolic disturbances, such as obesity, hyperglycemia, and aging.[9-16] A large body of evidence indicates that both intrinsic and extrinsic factors drive the hematopoietic process; however, the cellular and molecular mechanisms underlying the metabolic regulation of hematopoiesis remain for the most part elusive.

In adults, the bone marrow (BM) microenvironment provides niches that support the renewal, quiescence, and differentiation of hematopoietic stem and progenitor cells (HSPC).[17-19]

Recent studies have started to unveil the complexity and heterogeneity of niche cell types, niche factors, and their actions. BM mesenchymal stem cells [BMSC,

Correspondence:

RUAN HAI-BIN
hruan@umn.edu

Received: September 3, 2018.

Accepted: February 18, 2019.

Pre-published: February 21, 2019.

doi:10.3324/haematol.2018.205856

Check the online version for the most updated information on this article, online supplements, and information on authorship & disclosures: www.haematologica.org/content/104/9/1731

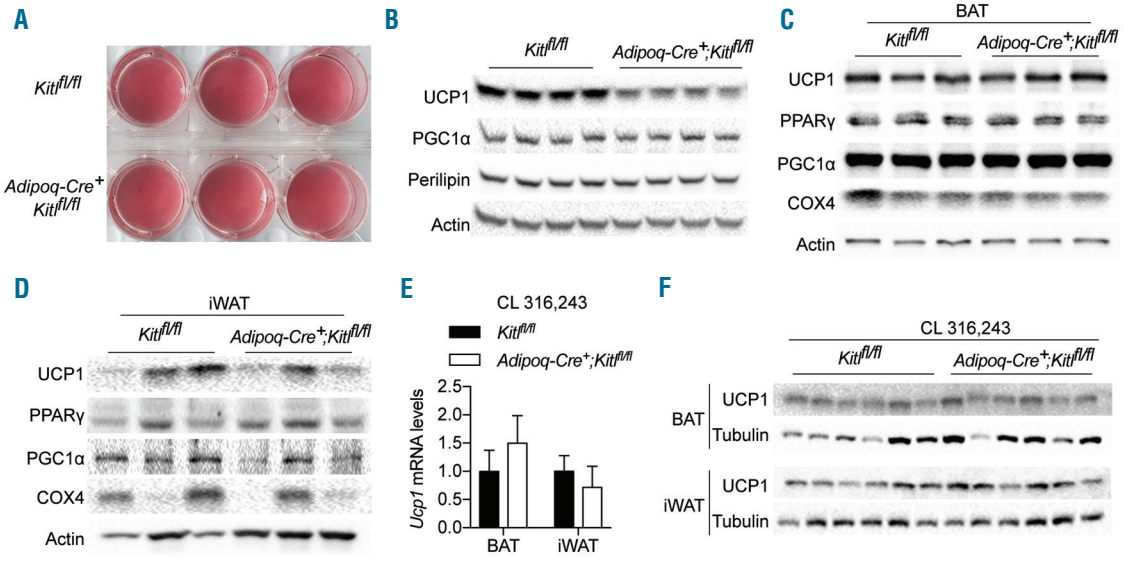

Figure 1. Role of adipose stem cell factor (SCF) in brown fat function. (A and B) Stromal vascular faction (SVF) cells from iWAT of *Kitl*$^{fl/fl}$ and *Adipoq-Cre*$^{+}$;*Kitl*$^{fl/fl}$ mice were differentiated into adipocytes *in vitro* and analyzed by Oil O Red staining (A) and western blotting (B). Densitometry of UCP1 shown in *Online Supplementary Figure S1C*. (C and D) Expression of proteins involved in adipogenesis and thermogenesis in BAT (C) and iWAT (D) from 7-week old *Kitl*$^{fl/fl}$ and *Adipoq-Cre*$^{+}$;*Kitl*$^{fl/fl}$ male mice. Densitometry of UCP1 shown in *Online Supplementary Figure S1D* and *E*. (E and F) *Kitl*$^{fl/fl}$ and *Adipoq-Cre*$^{+}$;*Kitl*$^{fl/fl}$ mice (n=6) were treated with CL 316,243 for seven days. *Ucp1* mRNA levels (E) and UCP1 protein levels (F) in BAT and iWAT were determined. Densitometry of UCP1 shown in *Online Supplementary Figure S1J and K*. Data are presented as mean±Standard Deviation.

also known as skeletal stem cells (SSC)] and their adipogenic, osteogenic, and chondrogenic progeny are major contributors of niche factors, such as stem cell factor (SCF) and CXC chemokine ligand 12 (CXCL12).[20-22] The sympathetic nervous system (SNS) extensively innervates the bone and BM to control hematopoietic homeostasis and regeneration *via* direct actions on HSPC and indirect actions on the niche.[23] In addition, signals from the vascular endothelial cells and the HSC progeny such as macrophages and megakaryocytes have also been shown to contribute to different aspects of HSPC regulation.[17] Nevertheless, whether these niche constituents mediate the sensing of metabolic cues and subsequent remodeling in hematopoiesis has not yet been determined.

White adipose tissue (WAT) that stores excess energy and brown adipose tissue (BAT) that dissipates energy as heat are key determinants of metabolic homeostasis. The role of BM adipose tissue (MAT), the third major adipose depot in the body, is just beginning to be revealed. Developmentally, BM adipocytes arise from the same Osterix^{+} skeletal lineage as osteoblasts and chondrocytes.[24-26] Anatomically, constitutive MAT (cMAT) is found in the most distal portion of the tibia and tail vertebrae while regulated MAT (rMAT) is found in the proximal skeletal sites.[27-29] Although cMAT is relatively stable, rMAT expands in conditions like obesity, diabetes, caloric restriction, and aging.[27-29] Functionally, there are tripartite interactions between MAT, bone, and hematopoiesis, yet their mechanistic characteristics are still not fully understood.[30] An early study taking advantage of the genetic and pharmacological inhibition of adipogenesis suggested MAT to be a negative regulator of the hematopoietic microenvironment.[31] In contrast, recent work demonstrated that MAT supports HSC regeneration and myeloerythroid maturation following irradiation and reconstitution, partially by secreting SCF.[32,33]

The close relationship between hematopoiesis and metabolism is also represented by their regulation by common growth factors and cytokines. SCF and its receptor KIT play an essential role in the survival, migration, and differentiation of multiple stem and progenitor cells including HSPC.[34] In the hematopoietic system, loss-of-function mutations in SCF/KIT cause macrocytic anemia while gain-of-function mutations lead to systematic mastocytosis, acute myeloid leukemia, and lymphoma.[35,36] In the bone marrow niche, SCF is expressed in LEPR^{+} stroma cells, endothelial cells, and adipocytes, but not in osteoblasts or hematopoietic cells.[22,32] Deleting SCF selectively in these positive niche cells leads to defects in HSC maintenance.[22,32] In the metabolic system, SCF has been shown to promote the differentiation of brown adipocytes from human pluripotent stem cells and to be essential to mitochondrial function and energy expenditure in mice.[37,38] However, the cellular source of SCF in regulating systemic metabolism has not been determined. Here, we investigated the contribution of adipose-derived SCF in regulating energy and glucose metabolism and in mediating the effect of metabolic stresses on unperturbed hematopoiesis.

Methods

Mice

All mice used in this study were purchased from the Jackson Laboratory, including *Kitl*$^{fl/fl}$ (stock n. 017861), *Adipoq-Cre* (stock n. 010803), *Osx1-Cre* (stock n. 006361), and *Kitl*^{EGFP} (stock n. 017860). All animals were kept on a 14 hour (h):10 h light:dark cycle in the animal facility at the University of Minnesota, Minneapolis, MN, USA. Mice were group-housed, with free access to water and either a standard chow diet or 60% high fat diet (Research Diets, D12492). 1 mg/kg BW of CL-316, 243 (R&D Systems, #1499,

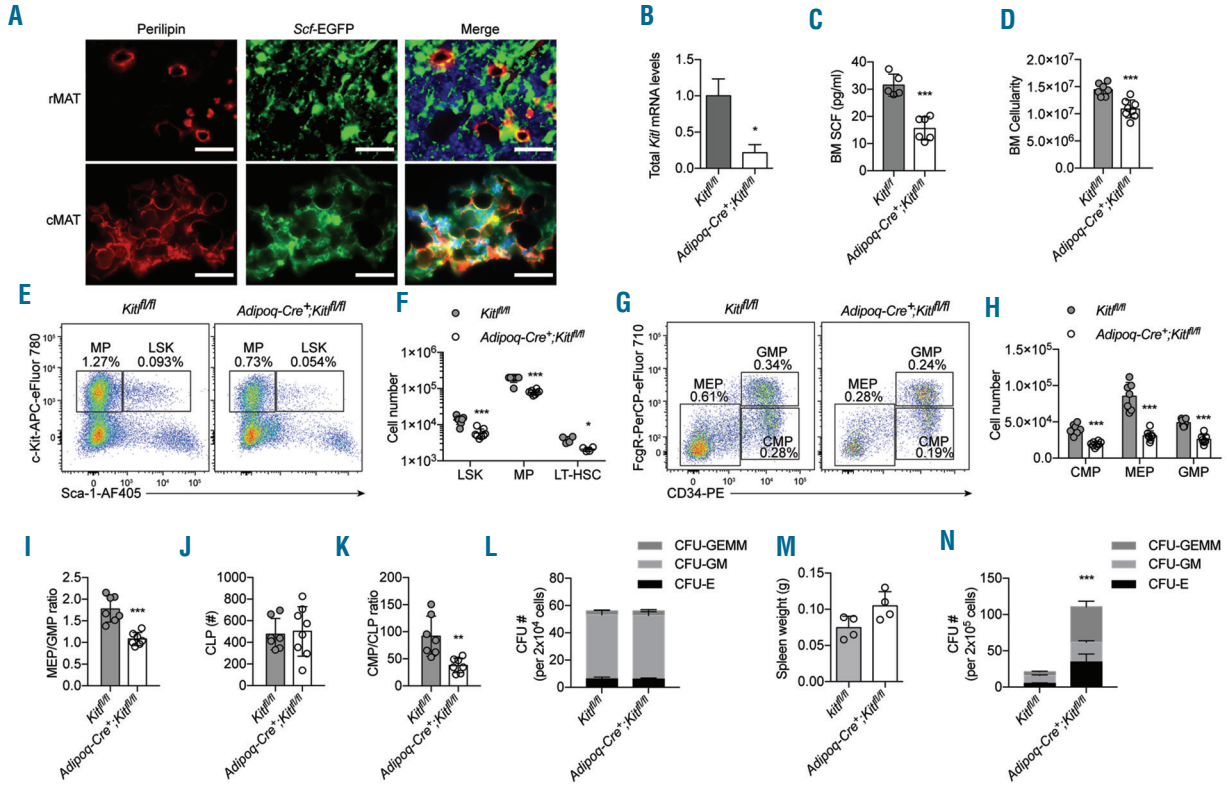

Figure 2. Adipocyte-derived stem cell factor (SCF) is a niche factor for hematopoietic stem and progenitor cells. (A) Co-staining of Perilipin and EGFP in the cMAT and rMAT of *Kitl*^{EGFP} mice. Scale bar=50 μm. (B and C) Levels of total *Kitl* mRNA (B) and SCF protein (C) in the flushed bone marrow (BM) from tibia of *Kitl*$^{fl/fl}$ (n = 5) and *Adipoq-Cre*$^{+}$;*Kitl*$^{fl/fl}$ (n=6) 13-week old male mice. (D) BM cellularity in the femur of 13-week old *Kitl*$^{fl/fl}$ (n = 7) and *Adipoq-Cre*$^{+}$;*Kitl*$^{fl/fl}$ (n=8) male mice. (E) Representative flow cytometry plots showing LSK and MP cells among the lineage^{-} CD127^{-} population in 13-week old *Kitl*$^{fl/fl}$ and *Adipoq-Cre*$^{+}$;*Kitl*$^{fl/fl}$ male mice. Average frequencies are shown as inserts. (F) Quantification of absolute numbers of LSK and MP cells in the femur of 13-week old *Kitl*$^{fl/fl}$ (n=7) and *Adipoq-Cre*$^{+}$;*Kitl*$^{fl/fl}$ (n=8) male mice and phenotypic LT-HSC in the femur of 8-month old *Kitl*$^{fl/fl}$ and *Adipoq-Cre*$^{+}$;*Kitl*$^{fl/fl}$ (n=4) male mice. (G) Representative flow cytometry plots showing CMP, MEP, and GMP cells among the MP population in 13-week old *Kitl*$^{fl/fl}$ and *Adipoq-Cre*$^{+}$;*Kitl*$^{fl/fl}$ male mice. Average frequencies are shown as inserts. (H) Absolute numbers of CMP, MEP, and GMP cells in the femur of 13-week old *Kitl*$^{fl/fl}$ (n=7) and *Adipoq-Cre*$^{+}$;*Kitl*$^{fl/fl}$ (n=8) male mice. (I) The ratio of marrow MEP to GMP in 13-week old *Kitl*$^{fl/fl}$ (n=7) and *Adipoq-Cre*$^{+}$;*Kitl*$^{fl/fl}$ (n=7) male mice. (J) The absolute number of CLP in 13-week old *Kitl*$^{fl/fl}$ (n=7) and *Adipoq-Cre*$^{+}$;*Kitl*$^{fl/fl}$ (n=7) male mice. (K) The ratio of marrow CMP to CLP in 13-week old *Kitl*$^{fl/fl}$ (n=7) and *Adipoq-Cre*$^{+}$;*Kitl*$^{fl/fl}$ (n=7) male mice. (L) Colony formation assay of 2x10^{4} BM cells from *Kitl*$^{fl/fl}$ and *Adipoq-Cre*$^{+}$;*Kitl*$^{fl/fl}$ (n=4) mice. (M) Spleen weight of *Kitl*$^{fl/fl}$ and *Adipoq-Cre*$^{+}$;*Kitl*$^{fl/fl}$ (n=4) mice. (N) Colony formation assay of 2x10^{5} splenic cells from *Kitl*$^{fl/fl}$ and *Adipoq-Cre*$^{+}$;*Kitl*$^{fl/fl}$ (n=4) mice. Data are presented as mean±Standard Deviation. *P<0.05; **P<0.01; ***P<0.001 by unpaired student t-test (B-K) or one-way ANOVA (N).

diluted in saline) were intraperitoneally (i.p.) injected when indicated. For thermoneutral housing, mice born at 22°C were transferred to a room maintained continuously at 30°C at the age indicated. All procedures involving animals were conducted within Institutional Animal Care and Use Committee guidelines under approved protocols.

Flow cytometry

Bone marrow cells were isolated by flushing the femur in Ca^{2+} and Mg^{2+} free PBS with 1% heat-inactivated bovine serum. Cells were dissociated to a single cell suspension by gently passing through a 25-gauge needle and then filtering through a 70-mm nylon mesh. Red blood cells from BM were removed by ammonium-chloride-potassium lysing buffer. For flow analyses, BM cells were stained with a cocktail of biotin-conjugated lineage antibodies CD3e, B220, Ter119, Mac-1 and Gr-1 (Biolegend, 133307), CD4 (Biolegend, 100403), CD5 (Biolegend, 100603), CD8 (Biolegend, 100703), followed by Streptavidin-AF488 (Biolegend, 405235). Cells were then stained with CD127-APC (eBioscience, 17-1271-82), c-Kit-APC-eFluor780 (eBioscience, 47-1171-82), Sca-1-Super Bright 436 (eBioscience, 62-5981-82), CD34-PE (Biolegend, 152204), and FcγR-PerCP-eFluor710 (eBioscience, 46-0161-80), CD150-BV605 (Biolegend, 115927), and CD48-BUV395 (BDBioscience, 740236). Multicolor analysis for progenitor and stem-cell quantification was performed on a 3-laser-LSRII flow cytometer (BD).[12,39] HSPC was defined as Lin^{-}Sca-1^{+}c-Kit^{+} (LSK); phenotypic LT-HSC was defined as CD150^{+}CD48^{-}Lin^{-}Sca-1^{+}c-Kit^{+}; myeloid progenitor (MP) was defined as Lin^{-}CD127^{-}Sca-1^{-}c-Kit^{+}; common lymphoid progenitor (CLP) was defined as Lin^{-}CD127^{+}Sca-1^{+}c-Kit^{+}; common myeloid progenitor (CMP) was defined as Lin^{-}CD127-Sca-1^{-}c-Kit^{+}CD34^{+} FcγR^{-}; megakaryocyte-erythrocyte progenitor (MEP) was defined as Lin^{-}CD127^{-}Sca-1^{-}c-Kit^{+}CD34^{-}FcγR^{-}; granulocyte-monocyte progenitor (GMP) was defined as Lin^{-}CD127^{-}Sca-1^{-}c-Kit^{+}CD34^{+}FcγR^{+}. SYTOX™ Green Dead Cell Stain (Thermo Fisher Scientific, S34860) was used to exclude dead cells. Absolute number was obtained by using counting beads (Thermo Fisher Scientific, C36950) as instructed by the manufacturer.

Metabolic assays

Body composition was assessed using an EchoMRI system by which fat and lean mass measured by magnetic resonance scanning were normalized to body weight for fat percentage and lean percentage. Adipose tissue weight was determined by dissecting and weighing indicated adipose depots. For glucose tolerance tests, 16 h-fasted mice were injected i.p. with glucose (1.5 g/kg

Table 1. Decline in production of mature blood cells in the periphery of *Adipoq-Cre*$^{+}$*;Kitl*$^{fl/fl}$ mice.

	13-week-old male		14-week-old female	
	Kitl$^{fl/fl}$ (n = 6)	*Adipoq-Cre+;Kitl*$^{fl/fl}$ (n = 9)	*Kitl*$^{fl/fl}$ (n = 8)	*Adipoq-Cre+;Kitl*$^{fl/fl}$ (n = 7)
RBC (x10^{12}/L)	10.54 ± 0.34	8.68 ± 0.28 ***	10.48 ± 0.40	8.83 ± 0.27 ***
HGB (g/L)	150.0 ± 3.7	137.6 ± 4.7 ***	152.0 ± 3.8	143.6 ± 4.5 **
Hematocrit L/L	0.493 ± 0.014	0.450 ± 0.015 ***	0.502 ± 0.026	0.463 ± 0.018 **
MCV (fL)	46.73 ± 0.50	51.91 ± 1.04 ***	47.89 ± 2.56	53.41 ± 2.28 ***
Reticulocyte (x10^{12}/L)	0.29 ± 0.28	0.34 ± 0.31 **	0.30 ± 0.04	0.43 ± 0.11 *
Platelet (x10^{9}/L)	1193.2 ± 115.6	987.6 ± 99.9 **	1027.8 ± 104.3	806.4 ± 82.2 ***
Neutrophil (x10^{9}/L)	0.90 ± 0.33	0.45 ± 0.20 *	0.87 ± 0.31	0.38 ± 0.17 **
Eosinophil (x10^{9}/L)	0.23 ± 0.10	0.10 ± 0.06 *	0.19 ± 0.11	0.13 ± 0.11
Basophil(x10^{9}/L)	0.04 ± 0.02	0.01 ± 0.01 *	0.04 ± 0.02	0.02 ± 0.01
Monocyte (x10^{9}/L)	0.06 ± 0.02	0.03 ± 0.01 *	0.13 ± 0.05	0.04 ± 0.01 ***
Lymphocyte (x10^{9}/L)	6.10 ± 2.08	3.71 ± 1.01 *	5.67 ± 1.38	3.73 ± 1.14 *

n: number; RBC: red blood cell counts; HGB: hemoglobin concentration; MCV: mean corpuscular volume. Data are presented as mean±Standard Deviation. *P<0.05; **P<0.01; ***P<0.001 by unpaired two-tailed t-test.

body weight). Blood glucose from tail-vein blood collected at the designated times was measured using a Bayer Contour Glucometer (9545C).

Cell culture

The stromal vascular faction (SVF) cells derived from iWAT were obtained as previously described.[38] SVF cells were cultured in DMEM/F12 (Corning, 10-090-CV) containing 10% FBS (GenClone, 25-514), 1% penicillin/streptomycin (Gibco, 10378016), 20 nM insulin (Sigma), and 1 nM triiodothyronine (T3, Sigma, T6397). Two days after becoming confluent (defined as Day 0), SVF cells were induced with DMEM/F12 containing 10% FBS, 1% penicillin/streptomycin, 0.5 mM isobutylmethylxanthine (IBMX, Sigma, I7018), 125 μM indomethacin (Sigma, I7378), 1 μM dexamethasone (Sigma, D4902), 20 nM insulin, and 1 nM T3 for 48 h. Cells were maintained in DMEM/F12 containing 10% FBS, 1% penicillin/streptomycin, 20 nM insulin, and 1 nM T3 until lipid drop appeared. This medium was replenished every two days.

Oil Red O staining

Cells were washed with PBS and then fixed with 10% formaldehyde (Sigma) for 1 h. After washing with 60% isopropanol, fixed cells were stained with Oil Red O solution (2 mg/mL in 60% isopropyl alcohol, Sigma, O-0625) for ten minutes (min), and rinsed five times with pure H_2O before photographic images were taken.

Genotyping and quantitative real-time polymerase chain reaction

Primers used for DNA amplification were: floxed-*Kitl*-F, CGAGGTAGGGGAAAAGAACC; floxed-*Kitl*-R, GGATCTTCCCAGAGGTTGGA; excised-*Kitl*-F, GGAAAAGAACCAAGTGAAGTC; excised-Kitl-R, ACGGGGAAAGACCTCCGGTCC; Adipoq-Cre-F, GGAAAAGAACCAAGTGAAGTC; Adipoq-Cre-R, ACGGGGAAAGACCTCCGGTCC. DNA for verifying knockout was isolated using the Quick-DNA Plus Kit (Zymo Research, #D4074). Genotyping was performed according to instructions in the manual provided by the Jackson Laboratory.

Total RNA from tissues was isolated using TRIzol (Invitrogen, 15596018). RNA was reverse-transcribed using iScript cDNA Synthesis Kits (Bio-Rad, 170-8891). Quantitative real-time polymerase chain reaction (qRT-PCR) was performed using SYBR Green Supermix (Bio-Rad, 1725124) with a C1000 Thermal Cycler (Bio-Rad) following the manufacturers' instructions. For thermal cycling: 95°C, 3 min; then 40 cycles of 95°C, 10 seconds (s) and 60°C, 30 s. The primers used for qRT-PCR were long *Kitl* (flanking exon 5 and 6): 5'-GCCAGAAACTAGATCCTTTACTCCTGA-3' and 5'-ACATAAATGGTTTTGTGACACTGACTCTG-3'; short *Kitl* (flanking junctions between exon 5/7 and exon 8/9): 5'-CCCGAGAAAGGGAAAGCCG-3' and 5'-ATTCTCTCTCTTTCTGTTGCAACATACTT-3'; total *Kitl* (flanking exon 2 and 3): 5'-TCTGCGGGAATCCTGTGACT-3' and 5'-CGGCGACATAGTTGAGGGTTAT-3'; excised *Kitl* (flanking exon 1 and 2, exon1 was floxed): 5'-CAGCGCTGCCTTTCCTTATGA-3' and 5'-ATCAGTCACAGGATTCCCGC-3', and the housekeeping gene 36b4: 5'-AGATGCAGCAGATCCGCAT-3' and 5'-GTTCTTGCCCATCAGCACC-3'. Delta-delta Ct analysis was used to calculate relative gene expression.

Histology and immunostaining

Long bones were fixed in 10% neutral buffered formalin followed by three days of decalcification in 14% EDTA, followed by paraffin or OCT embedding. Bones embedded in paraffin were sectioned at 5 μm thickness using a microtome (Olympus Cut 4060) and stained with Hematoxylin and Eosin (H&E). For quantification of the BM adipocytes, the BM areas 4.5 mm from growth plate were selected. Bones embedded in OCT were sectioned at 7 μm thickness using a cryostat (Leica). Sections were blocked with 3% bovine serum albumin, 0.2% TWEEN 20 in Tris-buffered saline, incubated with chicken-anti-GFP (Aves, GFP-1020, 1:1,000), rabbit-anti-perilipin (Cell Signaling Technology, #9349, 1:200) overnight, and secondary antibodies (Alexa Fluor 488 anti-Chicken IgG and Alexa Fluor 674 anti-Rabbit IgG, Life Technologies, 1:400) for 1 h. A Nikon system was used for fluorescence detection.

Western blot

Tissue proteins were extracted using RIPA buffer with freshly added proteinase inhibitors. Protein concentrations were determined using BCA Protein Assay Kit (Pierce). Equal amounts of protein samples were subjected to western blot. The following antibodies were used: anti-UCP1 (Abcam, ab209483, 1:5000 dilution), anti-PGC-1α (Bioworld, BS72263, 1:500 dilution), anti-PER-

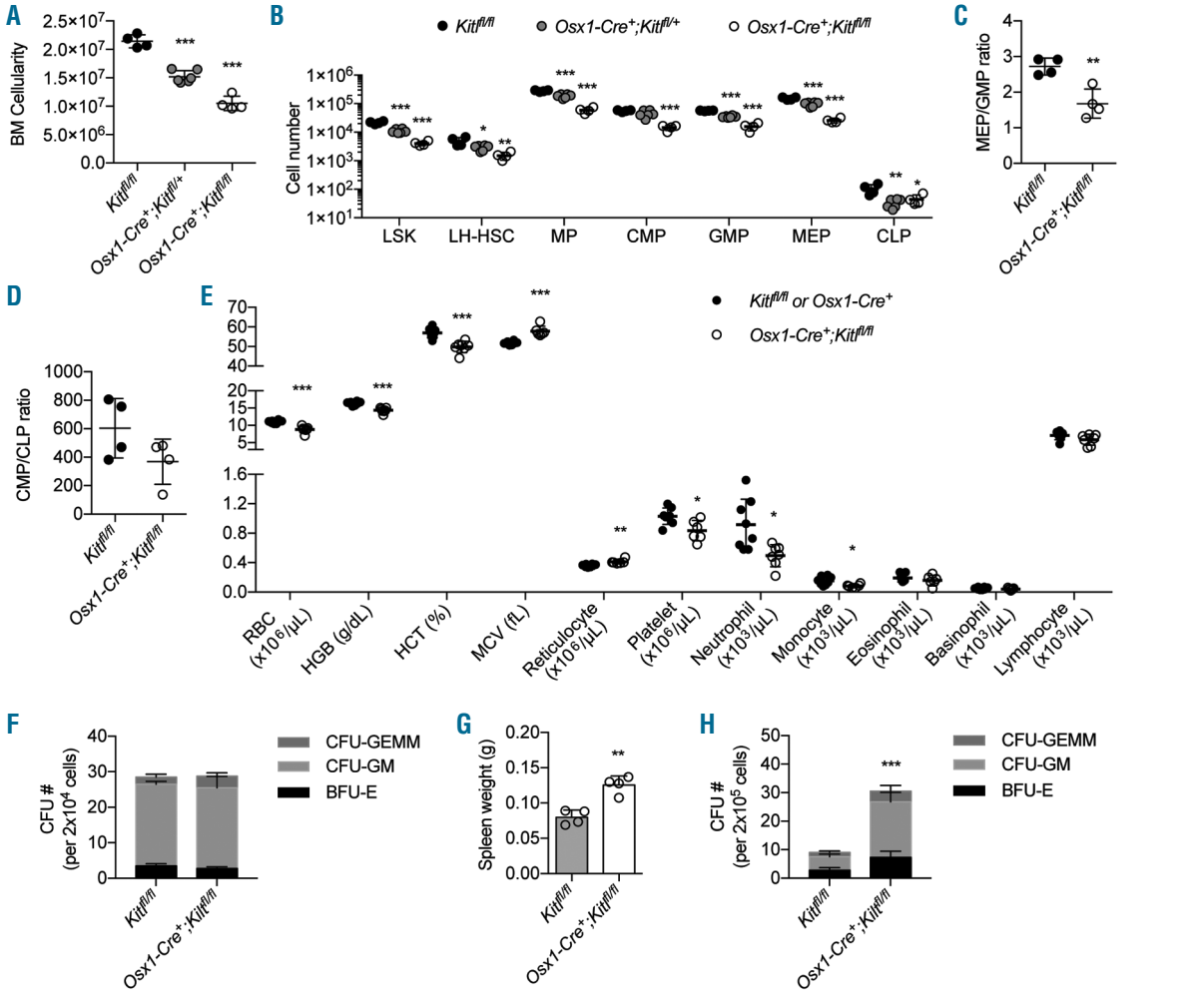

Figure 3. Impaired hematopoiesis when stem cell factor (SCF) is ablated in *Osx1*$^+$ cells. (A) Bone marrow cellularity in the femur of 8-month old control (n=4), *Osx1-Cre*$^+$*;Kitl*$^{fl/+}$ (n=5), and *Osx1-Cre*$^+$*;Kitl*$^{fl/fl}$ (n=4) male mice. (B) Frequencies of LSK, phenotypic LT-HSC, MP, CMP, GMP, MEP, and CLP populations in the bone marrow (BM) of 8-month old control (n=4), *Osx1-Cre*$^+$*;Kitl*$^{fl/+}$ (n=5), and *Osx1-Cre*$^+$*;Kitl*$^{fl/fl}$ (n=4) male mice, determined by flow cytometry. (C and D) Ratios of MEP to GMP (C) and CMP to CLP (D) in 8-month old control and *Osx1-Cre*$^+$*;Kitl*$^{fl/fl}$ (n=4) male mice. (E) Complete blood count of 10-week old control (n=8, including 6 *Kitl*$^{fl/fl}$ and 2 *Osx1-Cre*$^+$) and *Osx1-Cre*$^+$*;Kitl*$^{fl/fl}$ (n=7) male mice. (F) Colony formation assay of 2x10^4 BM cells from *Kitl*$^{fl/fl}$ and *Osx1-Cre*$^+$*;Kitl*$^{fl/fl}$ (n=4) mice. (G) Spleen weight of *Kitl*$^{fl/fl}$ and *Osx1-Cre*$^+$*;Kitl*$^{fl/fl}$ (n=4) mice. (H) Colony formation assay of 2x10^5 splenic cells from *Kitl*$^{fl/fl}$ and *Osx1-Cre*$^+$*;Kitl*$^{fl/fl}$ (n=4) mice. Data are presented as mean±Standard Deviation. **P*<0.05; ***P*<0.01; ****P*<0.001 by one-way ANOVA followed with Tukey's multiple comparison (A, B, and H) or unpaired Student *t*-test (C, E, and G).

ILIPIN (Cell Signaling Technology, 9349T, 1:1000 dilution), anti-PPARγ (CusAb, CSB-PA018424LA01HU, 1:500 dilution), anti-COX4 (Proteintech, 11242-1-AP, 1:1000 dilution), and anti-ACTIN (Sigma, A5441, 1:5000 dilution). Densitometry was performed using Image J. Relative band density was calculated by dividing the densitometry of target protein with loading control from the same membrane.

Isolation of bone marrow adipocytes and supernatant

A 0.6 mL microcentrifuge tube was cut open at the bottom and placed into a 1.5 mL microcentrifuge tube. Long bones were snipped both ends and placed in the prepared 0.6 mL microcentrifuge tube. BM was flowed out by quick centrifuge (from 0 to 10,000 rpm, RT). Red blood cells from BM were lysed by ammonium-chloride-potassium lysing buffer. After 3,000 rpm centrifugation for 5 min at RT, floating adipocytes were collected as BM adipocytes from the top layer.[40] The middle layer was collected and remaining cells were spun down by centrifugation (12,000 rpm, 30 s, RT). The supernatant was collected for SCF measurement using an ELISA (Thermo Fisher Scientific, EMKITL).

Colony-forming unit assay

The colony-forming unit (CFU) assay was performed using MethoCult™ GF M3434 (Stem cell) according to the manufacturer's instructions. Briefly, BM cells were flushed from one femur, and filtered through a 40 um cell strainer. Spleen was minced and pressed through a 40 um cell strainer to obtain single cell suspension. 2x10^4 BM cells or 2x10^5 spleen cells were plated in methylcellulose, and the CFU were counted after 12 days.

Statistical analysis

All data are presented as mean±Standard Deviation (SD) or mean±Standard Error of Mean (SEM) as indicated in the figure legends. The statistical significance between two groups was determined by unpaired two-tailed Student *t*-test (Microsoft Excel or GraphPad Prism 7). Datasets involving more than two groups were assessed by one-way ANOVA with Tukey's correction for multiple comparisons using GraphPad Prism 7. Two-way ANOVA followed by Tukey's correction or Sidak's correction for multiple comparisons was performed using GraphPad Prism 7 to examine data with two independent variables. **P*<0.05; ***P*<0.01; ****P*<0.001.

Results

Adipocyte-derived stem cell factor is not essential for brown fat function *in vivo*

To determine whether adipocyte-derived SCF cell-autonomously regulates BAT function *in vivo*, we generated fat-specific SCF KO mice by crossing *Adiponectin (Adipoq)-Cre* mice with *Kitl*$^{fl/fl}$ mice. The adipose stromal vascular faction (SVF) cells derived from *Kitl*$^{fl/fl}$ controls and *Adipoq-Cre*$^{+}$*;Kitl*$^{fl/fl}$ KO mice were isolated and differentiated into adipocytes in culture. The *Kitl* gene was specifically deleted (*Online Supplementary Figure S1A*) and the *Kitl* mRNA reduced its level (*Online Supplementary Figure S1B*) in KO cells when *Adipoq-Cre* started to be expressed after adipogenic induction (*Online Supplementary Figure S1B*). Control and KO SVF cells showed similar capacity in adipogenic differentiation, determined by Oil Red O staining (Figure 1A). Consistent with the previous finding that SCF is required for UCP1 expression,[37] we found that differentiated brown adipocytes from *Adipoq-Cre*$^{+}$*;Kitl*$^{fl/fl}$ mice had much lower levels of UCP1 protein compared to *Kitl*$^{fl/fl}$ cells (Figure 1B and *Online Supplementary Figure S1C*). Expression of PGC-1α and PERILIPIN was unaffected (Figure 1B).

We then sought to determine gene expression in thermogenic fat tissues *in vivo*. The levels of UCP1, PGC-1α, COX4, and PPARγ proteins in BAT and inguinal WAT (iWAT) were essentially the same between *Kitl*$^{fl/fl}$ and *Adipoq-Cre*$^{+}$*;Kitl*$^{fl/fl}$ mice (Figure 1C and D and *Online Supplementary Figure S1D and E*). *Kitl*$^{fl/fl}$ and *Adipoq-Cre*$^{+}$*;Kitl*$^{fl/fl}$ mice had similar body weight at 7, 14, and 28 weeks of age (*Online Supplementary Figure S1F-H*). No changes in the mass of BAT, iWAT, and gonadal WAT (gWAT) (*Online Supplementary Figure S1F*), composition of lean and fat mass (*Online Supplementary Figure S1G*), or fasting body weight (*Online Supplementary Figure S1H*) were observed. In addition, systemic glucose metabolism shown by the glucose tolerance test was also comparable between the two genotypes (*Online Supplementary Figure S1I*).

To assess sympathetic nerve-activated adaptive thermogenesis, we treated mice with a β3-adrenoceptor agonist, CL 316,243 for seven days. qRT-PCR and western blotting showed no difference in levels of *Ucp1* mRNA (Figure 1E) or UCP1 protein (Figure 1F and *Online Supplementary Figure S1J and K*) in BAT or iWAT between *Kitl*$^{fl/fl}$ and *Adipoq-Cre*$^{+}$*;Kitl*$^{fl/fl}$ mice. Together, these data demonstrate that SCF secreted by adipocytes is essential for UCP1 expression *in vitro* but is not essential for energy metabolism *in vivo*. It is possible that SCF from non-adipose cells or tissues may compensate for the loss of SCF in adipocytes, as no change in serum levels of SCF was observed in *Adipoq-Cre*$^{+}$*;Kitl*$^{fl/fl}$ mice (*Online Supplementary Figure S1L*).

Adipocyte-derived stem cell factor controls steady-state hematopoiesis

Marrow adipose tissue is an endocrine organ important for hematopoiesis and systemic metabolism.[27-30] MAT promotes the regeneration of hematopoietic stem cells after irradiation by secreting SCF.[32] We first confirmed that most BM adipocytes (approx. 77% in cMAT and approx. 80% in rMAT) expressed SCF by performing perilipin immunofluorescent staining on bone sections of *Kitl*^{EGFP} knockin mice (Figure 2A and *Online Supplementary Figure S2A*). Compared to BAT and iWAT, the flushed BM expressed similar levels of the long isoform of *Kitl* that can be transcribed and cleaved into the soluble form of SCF, but much less of the short *Kitl* transcript that encodes the membrane-bound SCF (*Online Supplementary Figure S2B*).[34] Note that there are significant numbers of non-adipocytes in the adipose tissues and BM analyzed. In BM, *Adipoq-Cre* was recently shown to only label mature adipocytes, but not bone stroma, adipogenic progenitors, hematopoietic cells, bone lining cells, or osteoblast cells.[41] In *Adipoq-Cre*$^{+}$*;Kitl*$^{fl/fl}$ mice, the *Kitl* gene was specifically knocked down in marrow adipocytes (*Online Supplementary Figure S2C*). We could observe a significant loss of *Kitl* transcript in the flushed BM (Figure 2B) and SCF protein in the BM supernatant (Figure 2C), suggesting that MAT is a major source of SCF in the BM.

We then quantified hematopoietic stem and progenitor cells (HSPC) in the BM of *Adipoq-Cre*$^{+}$*;Kitl*$^{fl/fl}$ mice by flow cytometry (*Online Supplementary Figure S3*).[12,39] We first characterized the *Adipoq-Cre*$^{+}$ line and could not observe any potential Cre-specific defects in BM cellularity or HSPC numbers when compared to wild-type mice (*Online Supplementary Figure S4*). Thus, *Kitl*$^{fl/fl}$ mice were used as controls for comparison in the following experiments. Loss of SCF specifically in adipocytes reduced marrow cellularity in male mice (Figure 2D). The frequency and also absolute number of lineage^{-}Sca^{-}1^{+}c-Kit^{+} (LSK) HSPC, phenotypic long-term (LT)-HSC (e.g. CD150^{+}CD48^{-} LSK cells), and myeloid progenitors (MP) were all down-regulated in *Adipoq-Cre*$^{+}$*; Kitl*$^{fl/fl}$ male mice (Figure 2E and F). Within MP, common myeloid progenitors (CMP), megakaryocyte-erythrocyte progenitors (MEP), and granulocyte-monocyte progenitors (GMP) all showed decreased frequency and number (Figure 2G and H). Interestingly, there was a reduction in the ratio of MEP to GMP (Figure 2I), suggesting that the extent of dependence on SCF varies between different myeloid progenitors. On the other hand, common lymphoid progenitors (CLP) maintained their number (Figure 2J) and the ratio of CMP/CLP was reduced (Figure 2K) in *Adipoq-Cre*$^{+}$*;Kitl*$^{fl/fl}$ mice. Colony formation assay showed that BM HSPC, though reducing their numbers in the SCF-deficient environment, did not show functional decline when assessed in a complete medium *in vitro* (Figure 2L). It suggests that loss of adipose SCF results in defects in the niche environment but not intrinsically in HSPC. Whether BM adipocyte-derived SCF supports the long-term proliferation and self-renewal of HSPC requires future investigation. Hematopoietic stresses can mobilize HSPC outside the BM to sites like the spleen to expand hematopoiesis.[42] We found that spleen in *Adipoq-Cre*$^{+}$*;Kitl*$^{fl/fl}$ mice was slightly heavier (Figure 2M) and splenic cells from *Adipoq-Cre*$^{+}$*;Kitl*$^{fl/fl}$ mice formed significantly more colony-forming units (CFU) *in vitro* (Figure 2N), indicating a compensatory induction of splenic hematopoiesis when BM hematopoiesis was defective.

Similar phenotypes were observed in female mice. There was a trending decline in BM cellularity in *Adipoq-Cre+;Kitl*$^{fl/fl}$ female mice, compared to their control counterparts (*Online Supplementary Figure S5A*). Both the absolute number and frequency of LSK cells, MP, CMP, MEP, and GMP were declined when SCF was absent (*Online Supplementary Figure S5B and C*). CLP remained unchanged (*Online Supplementary Figure S5B and C*). *Adipoq-Cre*$^{+}$*;Kitl*$^{fl/fl}$ female mice also had reduced ratio of MEP to GMP (*Online Supplementary Figure S5D*). These data demon-

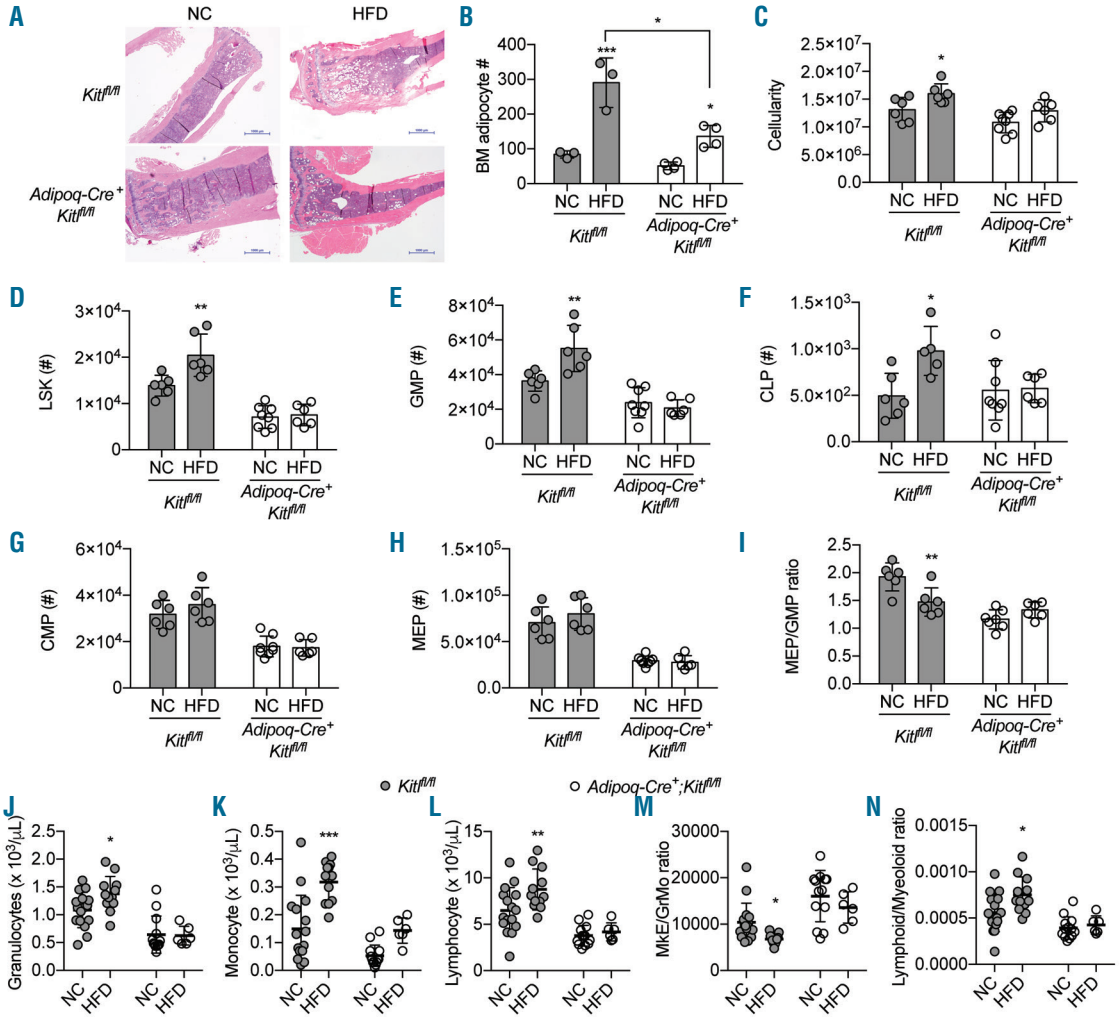

Figure 4. High-fat diet (HFD)-stressed hematopoiesis in control and *Adipoq-Cre*⁺;*Kitl*$^{fl/fl}$ male mice. (A and B) *Kitl*$^{fl/fl}$ and *Adipoq-Cre*⁺;*Kitl*$^{fl/fl}$ male mice at the age of eight weeks were fed with normal chow (NC) or HFD (n=3-4) for another eight weeks. (A) Representative images of femur sections. (B) Quantification of adipocyte numbers in the BM from the growth plate to 4.5 mm away distally. (C-I) 8-week old *Kitl*$^{fl/fl}$ (n=6 for each diet) and *Adipoq-Cre*⁺;*Kitl*$^{fl/fl}$ (n=8 for NC and n=6 for HFD) male mice were fed with NC or HFD for eight weeks. BM cellularity (C), LSK number (D), GMP number (E), CLP number (F), CMP number (G), MEP number (H), and the MEP/GMP ratio (I) were determined by flow cytometry. (J-N) Complete blood count of NC- and HFD-fed *Kitl*$^{fl/fl}$ (n=16 and 13, respectively) and *Adipoq-Cre*⁺;*Kitl*$^{fl/fl}$ (n=12 and 6, respectively) male mice showing granulocyte number (J), monocyte number (K), lymphocyte number (L), megakaryocyte-erythrocyte (MkE) to granulocyte-monocyte (GrMo) ratio (M), and the ratio of lymphocyte to all myeloid cells including MkE and GrMo (N). Data are presented as mean±Standard Deviation. **P*<0.05; ***P*<0.01; ****P*<0.001 by two-way ANOVA followed by multiple comparison using Tukey's correction (B) or Sidak correction (C-N).

strate that adipocyte-derived niche factor SCF is essential for the maintenance of hematopoietic stem and myeloid progenitor cells.

We then performed the complete blood count test of the peripheral blood. Levels of red blood count (RBC), hemoglobin concentration (HGB), and hematocrit were all decreased in both male and female *Adipoq-Cre*⁺;*Kitl*$^{fl/fl}$ mice when compared to *Kitl*$^{fl/fl}$ controls (Table 1). The mean corpuscular volume (MCV) and the count of reticulocytes were both significantly increased in *Adipoq-Cre*⁺;*Kitl*$^{fl/fl}$ mice (Table 1), showing that *Adipoq-Cre*⁺;*Kitl*$^{fl/fl}$ mice developed the typical macrocytic anemia that is observed in animals and patients with loss-of-function mutations in the SCF/KIT pathway.[35,36,43] Meanwhile, *Adipoq-Cre*⁺;*Kitl*$^{fl/fl}$ mice also had less platelets compared to control mice (Table 1). Within white blood cells, neutrophils, monocytes, and lymphocytes reduced their number in both sexes, while eosinophils and basophils were significantly declined in male *Adipoq-Cre*⁺;*Kitl*$^{fl/fl}$ mice and showed a trending reduction in female *Adipoq-Cre*⁺;*Kitl*$^{fl/fl}$ mice (Table 1). Taken together, these data from both male and female mice indicate that adipocytes compose a niche that produce SCF to maintain unperturbed hematopoiesis.

Ablation of stem cell factor in Osterix⁺ cells impairs hematopoiesis

Adipoq-Cre-mediated ablation deleted SCF in all adipose tissues. To exclude the potential confounding effect of SCF from peripheral adipose tissues, we then conditionally deleted the *Kitl* gene in BM stroma cells using the *Osterix (Osx1)-Cre*, which marks progenitor cells that can be differentiated into MAT.[24-26] Loss of SCF in Osx1⁺ cells resulted in lower BM cellularity (Figure 3A) and drastically reduced populations of LSK, phenotypic LT-HSC, MP, CMP, GMP, MEP, and CLP in *Osx1-Cre*⁺;*Kitl*$^{fl/fl}$ mice (Figure 3B). Such reductions were much larger than those

observed in *Adipoq-Cre*$^{+}$*;Kitl*$^{fl/fl}$ mice (Figure 2), suggesting that SCF from non-MAT, *Osx1-Cre*-derived niche cells also contributed to HSPC defects in *Osx1-Cre*$^{+}$*;Kitl*$^{fl/fl}$ mice. Interestingly, heterozygous *Osx1-Cre*$^{+}$*;Kitl*$^{fl/+}$ mice also had decreased BM cellularity and frequencies of all HSPC (Figure 3A and B), suggesting the haploinsufficiency of SCF in hematopoietic regulation. Similar to findings in *Adipoq-Cre*$^{+}$*;Kitl*$^{fl/fl}$ mice, the MEP/GMP ratio was reduced (Figure 3C) and the CMP/CLP ratio showed a trending decrease (Figure 3D). As a result, *Osx1-Cre*$^{+}$*;Kitl*$^{fl/fl}$ mice suffered macrocytic anemia (Figure 3E). Furthermore, there were fewer platelets, neutrophils, and monocytes in *Osx1-Cre*$^{+}$*;Kitl*$^{fl/fl}$ mice (Figure 3E). Counts of eosinophils, basophils, and lymphocytes were similar between control and *Osx1-Cre*$^{+}$*;Kitl*$^{fl/fl}$ mice (Figure 3E). BM cells from *Osx1-Cre*$^{+}$*;Kitl*$^{fl/fl}$ KO mice could efficiently form CFU as wild-type controls (Figure 3F). suggesting defects in the niche environment not intrinsically in HSPC as a result of loss of adipose SCF. However, splenomegaly and profoundly increased CFU formation of splenic cells were observed in *Osx1-Cre*$^{+}$*;Kitl*$^{fl/fl}$ mice (Figure 3G and H), demonstrating a shift of hematopoiesis toward the spleen. Taking data from *Adipoq-Cre*- and *Osx1-Cre*-mediated knockout mice, we argue that, in the steady-state, SCF from MAT is essential for homeostasis of hematopoietic progenitors.

MAT-derived stem cell factor contributes to stressed hematopoiesis in obesity

Obesity is associated with increased MAT mass and altered hematopoietic and immune functions. We then asked whether MAT-derived SCF mediates the effect of high-fat diet (HFD) on hematopoiesis. Male *Kitl*$^{fl/fl}$ and *Adipoq-Cre*$^{+}$*;Kitl*$^{fl/fl}$ mice gained similar body weight after HFD feeding for eight weeks (*Online Supplementary Figure S6A*). HFD significantly increased BM adiposity and cellularity, which could be slightly diminished by the loss of adipose SCF (Figure 4A-C). We did not observe any changes in *Kitl* gene expression or SCF secretion after HFD in the BM (*Online Supplementary Figure S6B and C*), indicating a potential compensation from non-adipocytes. Future experiments are required to determine SCF expression by different stroma cells during HFD. Flow cytometric assessment of HSPC showed that numbers of LSK, GMP, and CLP progenitors in wild-type male mice were increased after HFD (Figure 4D-F). Such induction was completely blunted in *Adipoq-Cre*$^{+}$*;Kitl*$^{fl/fl}$ males (Figure 4D-F). It is possible that other yet-to-be defined factors mediate the expansion of HSPC in response to HFD, but their complete function requires MAT-secreted SCF. Even though HFD did not affect numbers of CMP or MEP (Figure 4G and H), there was a reduction in the ratio of MEP to GMP (Figure 4I). The MEP/GMP ratio was lower in *Adipoq-Cre*$^{+}$*;Kitl*$^{fl/fl}$ males and could not be further reduced by HFD (Figure 4I). Consistent with the changes of HSPC in the BM, there was an increase in the number of granulocytes, monocytes, and lymphocytes in the peripheral blood of wild-type males after HFD (Figure 4J-L). The ratio of megakaryocyte (represented by platelet)-erythrocyte (MkE) to granulocyte-monocyte (GrMo) was down-regulated (Figure 4M), while the ratio of lymphocytes to all myeloid cells was up-regulated by HFD (Figure 4N). These data suggest that HFD preferentially promotes the hematopoietic differentiation toward the GrMo and lymphoid lineages, which may contribute to the development of inflammation and insulin resistance in obesity. In the peripheral blood of *Adipoq-Cre*$^{+}$*;Kitl*$^{fl/fl}$ male mice, however, HFD could not increase the number of granulocytes, monocytes or lymphocytes to the extent observed in *Kitl*$^{fl/fl}$ males (Figure 4J-L). HFD-induced downregulation of MkE/GrMo ratio and upregulation of lymphoid/myeloid lineage ratio were both ablated in *Adipoq-Cre*$^{+}$*;Kitl*$^{fl/fl}$ male mice (Figure 4M and N). Other peripheral blood parameters including RBC count, HGB, MCV, and platelet count were either not affected by HFD or were similarly regulated between *Kitl*$^{fl/fl}$ and *Adipoq-Cre*$^{+}$*;Kitl*$^{fl/fl}$ males (*Online Supplementary Figure S6D*). These results indicate that SCF from MAT is required for the skewed hematopoietic differentiation toward GrMo and lymphoid lineages during HFD.

Sexual dimorphism is observed in obesity-associated inflammation and immune dysfunction, which is partially attributable to difference in hematopoiesis.[44,45] We then sought to determine the effect of MAT-derived SCF on obesity-stressed hematopoiesis in females. HFD-induced gain in body weight was similar between *Kitl*$^{fl/fl}$ and *Adipoq-Cre*$^{+}$*;Kitl*$^{fl/fl}$ female mice (*Online Supplementary Figure S7A*). We found that, compared to males, HFD feeding in wild-type females did not affect BM cellularity (*Online Supplementary Figure S7B*) but LSK and all myeloid progenitors including CMP, MEP and GMP were all expanded (*Online Supplementary Figure S7C-F*), without a change in the relative ratio of MEP to GMP (*Online Supplementary Figure S7G*). The increase in the frequency of LSK, CMP, and MEP by HFD in females was abolished when SCF was deleted in adipocytes (*Online Supplementary Figure S7C-E*). However, the increase in GMP frequency after HFD in females seemed to be independent of adipocyte-derived SCF (*Online Supplementary Figure S7F*). In the peripheral blood, HFD feeding significantly augmented the red blood cell count and hemoglobin concentration in both *Kitl*$^{fl/fl}$ and *Adipoq-Cre*$^{+}$*;Kitl*$^{fl/fl}$ female mice (*Online Supplementary Figure S7H and I*). Mean corpuscular volume (MCV), platelet count, and lymphocyte count were not affected by HFD in either *Kitl*$^{fl/fl}$ or *Adipoq-Cre*$^{+}$*;Kitl*$^{fl/fl}$ female mice (*Online Supplementary Figure S7J-L*). Despite the increased frequency of GMP in the BM, there was a declining trend in peripheral granulocytes and significant downregulation of monocytes in HFD wild-type females, which was absent in *Adipoq-Cre*$^{+}$*;Kitl*$^{fl/fl}$ female mice (*Online Supplementary Figure S7M and N*). Reasons causing these discrepancies between the BM and the periphery are unclear, but may involve the production and turnover of mature cells, their release into the circulation, and recruitment to target tissues. Taken all these data from male and female mice, we conclude that MAT niche factor SCF is required for HFD-induced changes in HSPC maintenance and differentiation, despite the sex differences observed in such responses.

Adipocyte-derived stem cell factor partially mediates the β3-adrenergic regulation of hematopoietic stem and progenitor cells

The BM is extensively innervated by the SNS.[23,46] β-adrenoceptors are expressed in Nestin^{+} SSC and their activation by the SNS mediates the circadian mobilization of HSC,[47,48] while the neuropathy of the BM niche contributes to the pathogenesis of myeloproliferative neoplasms.[49,50] In addition, MAT, particularly the rMAT, expresses all three β-adrenoceptors and undergoes remodeling when the sympathetic tone is elevated by cold or

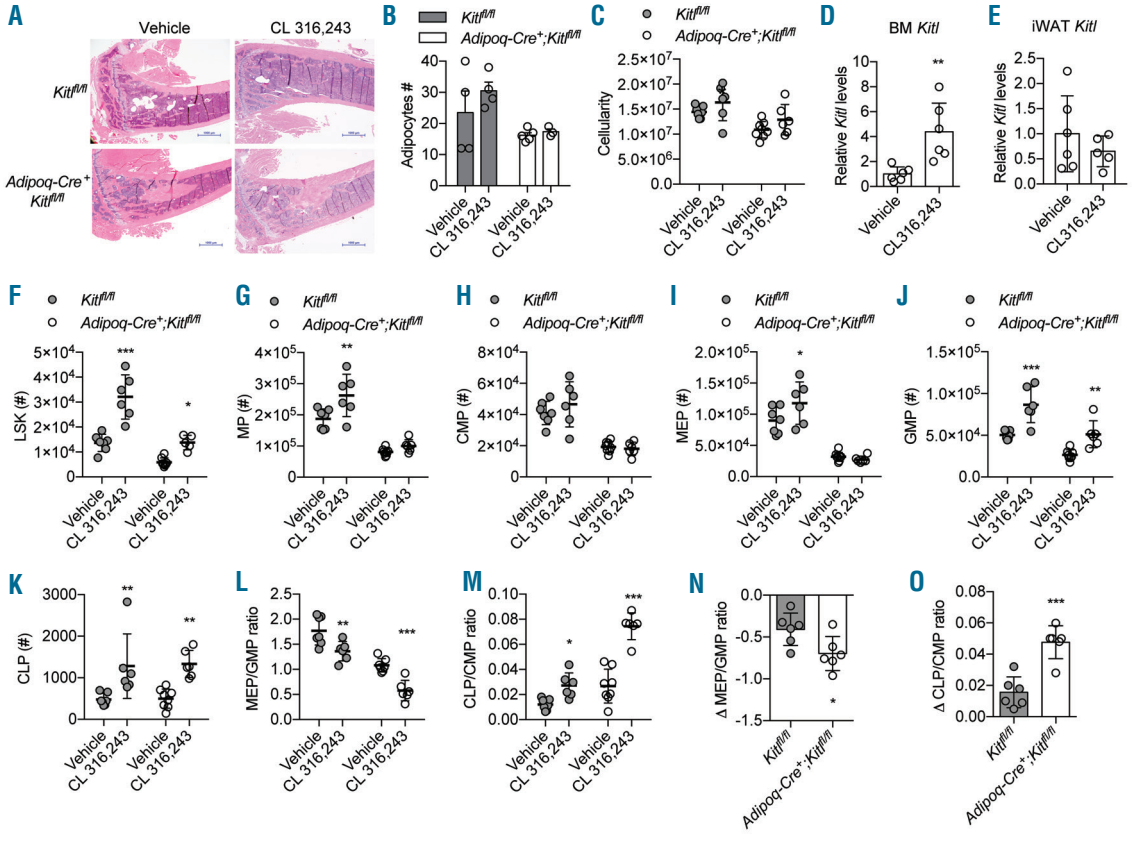

Figure 5. Sympathetic nervous system (SNS)-activated hematopoiesis in control and *Adipoq-Cre*$^{+}$*;Kitl*$^{fl/fl}$ mice. (A and B) 12-week old *Kitl*$^{fl/fl}$ and *Adipoq-Cre*$^{+}$*;Kitl*$^{fl/fl}$ male mice were treated with the saline vehicle or CL 316,243 for one week. (A) Representative images of femur sections. (B) Quantification of adipocyte numbers in the bone marrow (BM) from the growth plate to 4.5 mm away distally. (C) BM cellularity of 12-week old *Kitl*$^{fl/fl}$ (n=7 for vehicle and n=6 for CL) and *Adipoq-Cre*$^{+}$*;Kitl*$^{fl/fl}$ (n=8 for vehicle and n=6 for CL) male mice were treated with the saline vehicle or CL 316,243 for one week. (D and E) Relative *Kitl* mRNA levels in the BM (D) or iWAT (E) of wild-type mice treated with vehicle or CL 316,243 (n=6) for one week. (F-M) 12-week old *Kitl*$^{fl/fl}$ (n=7 for vehicle and n=6 for CL) and *Adipoq-Cre*$^{+}$*;Kitl*$^{fl/fl}$ (n=8 for vehicle and n=6 for CL) male mice were treated with the saline vehicle or CL 316,243 for one week. LSK number (F), MP number (G), CMP number (H), MEP number (I), GMP number (J), CLP number (K), the MEP/GMP ratio (L), and the CLP/CMP ratio (M) were determined by flow cytometry. (N and O) CL 316,243 treatment-induced changes in MEP/GMP ratio (N) and CLP/CMP ratio (O) in *Kitl*$^{fl/fl}$ (n=6) and *Adipoq-Cre*$^{+}$*;Kitl*$^{fl/fl}$ (n=6) male mice. Data are presented as mean±Standard Deviation. **P*<0.05; ***P*<0.01; ****P*<0.001 by two-way ANOVA followed by multiple comparison using Sidak correction (F-M) or unpaired, two-tailed Student *t*-test (D, N, and O).

β-adrenergic agonists.[51,52] We then sought to determine whether MAT-secreted SCF mediates the effect of β3-adrenergic signaling on hematopoiesis. Treatment with CL 316,243 to activate the β3-adrenoceptor for seven days did not change body weight, body fat percentage, MAT mass, or BM cellularity in either *Kitl*$^{fl/fl}$ or *Adipoq-Cre*$^{+}$*;Kitl*$^{fl/fl}$ mice, when compared to saline controls (Figure 5A-C and *Online Supplementary Figure S8A and B*). Scheller *et al.* recently showed that MAT, compared to peripheral WAT, relatively resists lipolysis and remodeling in response to CL 316,243.[51] We measured *Kitl* gene expression and found that CL 316,243 strongly induced *Kitl* mRNA in the BM but not iWAT (Figure 5D and E). *Adipoq* mRNA in MAT could be also induced by CL 316,243 (*Online Supplementary Figure S8C*), suggesting that β3-adrenergic activation is able to remodel MAT. CL 316,243 treatment significantly increased the numbers of LSK, MP, MEP, GMP, and CLP in the wild-type bone marrow (Figure 5F-K). Interestingly, the induction of LSK and MP, in particular MEP, by CL 316,243 was diminished in *Adipoq-Cre*$^{+}$*;Kitl*$^{fl/fl}$ mice (Figure 5F, G, and I). The number of CMP was not affected by CL 316,243 in either control or *Adipoq-Cre*$^{+}$*;Kitl*$^{fl/fl}$ mice (Figure 5H). CL 316,243-induced increase in GMP and CLP was not dependent on adipocyte-derived SCF (Figure 5J and K). As a result of the loss of adipose SCF, the reduction in MEP/GMP ratio was further decreased, while the increase in CLP/CMP ratio was further augmented in *Adipoq-Cre*$^{+}$*;Kitl*$^{fl/fl}$ mice upon CL 316,243 treatment (Figure 5L-O). These data indicate that SCF from MAT mediates some aspects of homeostatic responses in the BM upon the β3-adrenergic activation. Nonetheless, we cannot exclude the possibility that the role of CL 316,243 on hematopoiesis is affected by lipolysis in peripheral WAT.

Compared to the standard housing temperature (22°C), thermoneutrality (30°C) suppresses the SNS, promotes HSPC apoptosis, and increases the radiosensitivity of mice.[53] Consistent to the previous finding,[53] we did not observe any difference in BM cellularity (*Online Supplementary Figure S9A*) or the frequency of LSK, MP, and CLP (Online Supplementary Figure S9B) between mice housed at 22°C and 30°C. However, thermoneutrality increased the ratio of MEP to GMP and the ratio of CLP to CMP (*Online Supplementary Figure S9C and D*). After

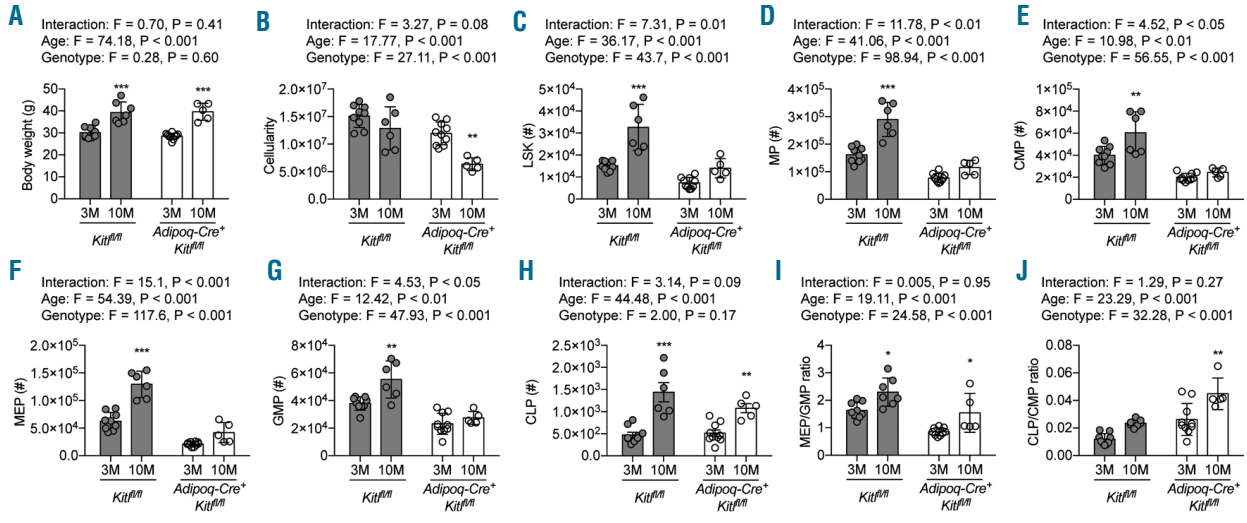

Figure 6. The effect of aging on hematopoietic stem and progenitor cells (HSPC) in *Kitfl/fl* and *Adipoq-Cre+;Kitfl/fl* mice. (A) Body weight of *Kitfl/fl* and *Adipoq-Cre+;Kitfl/fl* (n=6) male mice at three [n=9 and 10 for control and knock-out (KO), respectively] and ten (n=6 and 5 for control and KO, respectively) months of age. (B-J) Flow cytometric analyses of bone marrow from *Kitfl/fl* and *Adipoq-Cre+;Kitfl/fl* (n=6) male mice at three (n=9 and 10 for control and KO, respectively) and ten (n=6 and 5 for control and KO, respectively) months of age, showing total cellularity (B), LSK number (C), MP number (D), CMP number (E), MEP number (F), GMP number (G), CLP number (H), MEP/GMP ratio (I), and CLP/CMP ratio (J). Data are presented as mean±Standard Deviation. Two-way ANOVA followed by multiple comparison using Tukey's correction was performed. (Top) *P*-values for interaction and between groups. **P*<0.05; ***P*<0.01; ****P*<0.001 between 3M and 10M mice in indicated genotypes.

being housed at 30°C for one month, *Adipoq-Cre+;Kitfl/fl* mice had similar body weight, body composition, and MAT mass to *Kitfl/fl* mice (*Online Supplementary Figure S9E and F*). Loss of adipose SCF eliminated the rise in MEP/GMP ratio (*Online Supplementary Figure S9G*) but further augmented the increase in CLP/CMP ratio (*Online Supplementary Figure S9H*). Collectively, these data show that adipocyte-derived SCF mediates part of the environmental effects, particularly those *via* the β3-adrenergic signaling, on HSPC function.

MAT-provided stem cell factor in the aged hematopoietic stem and progenitor cell compartment

Aging-related changes in the hematopoietic system can be attributed to cell-intrinsic and microenvironmental alterations.[54] MAT expands as a function of age in both rodents and humans,[27] we then sought to determine whether SCF from MAT contributes to altered HSPC function during aging. Young (3 months old) and middle-aged (10 months old) male mice were analyzed; we did not observe any difference in body weight between *Kitfl/fl* and *Adipoq-Cre+;Kitfl/fl* mice at either age (Figure 6A). Aging slightly decreased BM cellularity in control mice, which was further down-regulated by the loss of adipose SCF (Figure 6B). Strikingly, the expansion of LSK and various myeloid progenitors including CMP, MEP, and GMP observed in middle-aged mice was totally abolished in *Adipoq-Cre+;Kitfl/fl* mice (Figure 6C-G). There were more CLP in 10-month old mice than in 3-month old mice, but there was no difference in these changes between genotypes (Figure 6H). Aging increased the ratios of both MEP to GMP and CLP to CMP; however, *Kitfl/fl* and *Adipoq-Cre+;Kitfl/fl* mice showed similar extent of increase as the interaction effect was not statistically significant (Figure 6I and J). These data demonstrate that SCF, as a MAT niche factor, is essential for the phenotypic expansion of HSC and myeloid progenitors during aging.

Discussion

Hematopoietic cytokines support the developmental processes of blood cells, at least partially through rewiring the cellular metabolism. Meanwhile, many of these cytokines also act directly on diverse metabolic tissues and cells. For example, erythropoietin improves glycemic control and insulin sensitivity, prevents obesity by acting on the hypothalamus, and attenuates adipose tissue inflammation.[55] Granulocyte-macrophage colony-stimulating factor regulates lipid metabolism in the liver.[56] Interleukin 4 inhibits adipogenesis, promotes lipolysis, and also disposes glucose by enhancing insulin action.[57,58] Interestingly, a specific hemopoietin cocktail composed of SCF, FLT3 ligand, IL-6, and vascular endothelial growth factor together with bone morphogenic protein 7 induces efficient differentiation of human pluripotent stem cells into functional brown adipocytes.[37] Our previous work showed that the expression of SCF in BAT is sensitive to food availability and environmental temperature.[38] SCF overexpression activates thermogenesis in BAT and reduces weight gain, while *Kit* mutant mice become obese as a result of reduced energy expenditure.[38] Consistently with these previous findings, in this study we found that adipose-derived SCF was required for thermogenic gene expression in cultured adipocytes, demonstrating a cell-autonomous effect of SCF. However, no changes in UCP1 expression, body weight, or glucose metabolism were observed in *Adipoq-Cre+;Kitfl/fl* mice, suggesting a possible

compensation from SCF or other factors secreted by non-adipose cells. Determining additional sources of SCF in regulating systemic metabolism is warranted in future studies.

In the BM, SCF is secreted by endothelial cells,[22] stromal cells that can be labeled by LEPR,[6,59] CXCL12,[60] Nestin-GFP^{low},[60] PDGFRa,[62] N-Cadherin,[63] and *Prx1-Cre*,[21] and adipocytes.[32] Loss of SCF from these niche cells all leads to reduced HSPC numbers.[64,65] It is still highly debatable whether osteoblasts express SCF, but HSC frequency and function were not affected by deleting SCF or CXCL12 from Col2.3$^+$ osteoblasts or ablating Ocn$^+$ osteoblasts cells.[21,22,66,67] A recent study by Zhou *et al.* elegantly showed that BM adipocytes proliferate after irradiation or chemotherapy, and deleting SCF using *Adipoq-Cre/ER* inhibits hematopoietic regeneration.[32] In this study, using *Adipoq-Cre*- and *Osx1-Cre*-mediated knockout of SCF, we determined that MAT-secreted SCF is essential for HSC maintenance and hematopoiesis also in the steady-state. Zhou *et al*. did not observe any deficiency in HSC frequency in non-irradiated *Adipoq-Cre/ER$^+$;Kitl$^{GFP/fl}$* mice, probably because they used heterozygous *Kitl$^{GFP/fl}$* mice as controls, in which the GFP insert disrupted one allele of the *Kitl* gene. Haploinsufficiency of the SCF/KIT pathway has been well documented,[22,36] and we also observed substantial defects in HSPC in heterozygous *Osx1-Cre$^+$;Kitl$^{fl/+}$* mice. The discrepancies between the results of our studies and those of Zhou *et al*. could also lie in the different Cre lines used. *Adipoq-Cre* only labels mature adipocytes, but not bone stroma, adipogenic progenitors, hematopoietic cells, bone lining cells, or osteoblast cells.[41] However, *Adipoq-CreER* also recombines in a subset of LEPR$^+$ stromal cells in the BM.[32] On the other hand, the *Adipoq-Cre* line has its limitations as the Cre expression is not restricted to adulthood. However, a minimal amount of MAT is present at the age of one week in mice and MAT rapidly expands afterwards.[52] We argue that the hematopoietic defects observed in adult *Adipoq-Cre$^+$;Kitl$^{fl/fl}$* mice were largely due to SCF excision during adulthood. In the BM of young mice, adipocytes are relatively rare, compared to other cell types that also express SCF. Even though more than half of *Kitl* mRNA and SCF protein were lost in the BM of *Adipoq-Cre$^+$;Kitl$^{fl/fl}$* mice, it is still unclear why such a profound effect could be observed when adipose SCF was absent. Note that we cannot rule out the contributions of peripheral adipocytes and other Osx1$^+$ progeny to the hematopoietic defects observed in *Adipoq-Cre$^+$;Kitl$^{fl/fl}$* mice and *Osx1-Cre$^+$;Kitl$^{fl/fl}$* mice, respectively. Tools that can selectively target MAT are needed to solve this enigma.

There have been a handful of studies that investigated the role of diet and obesity on the composition of the HSPC compartment and blood cell production.[9-13,15,16] Despite the inconsistencies seen in these studies, such as the different mouse models, diets, and length of treatment employed, it is generally accepted that diet-induced obesity promotes the immediate expansion of LSK stem cells but push their differentiation skewed toward the myeloid and lymphoid lineages, which will result in long-term defects in hematopoiesis upon stress and infection. Of note, only male mice were assessed in these studies. Here, we consistently found that HFD activates myelopoiesis and lymphopoiesis in male mice, which may facilitate tissue inflammation in obesity. However, HFD in females did not change the ratio of MEP to GMP in the BM or the MkE/GrMo ratio in the peripheral blood. These discrepancies may help explain the sexual dimorphism in metabolic dysfunction associated with obesity in animals and humans. It has recently been reported that estrogen signaling could control the sexual dimorphism of HSPC development.[44,45] Shown in this study, HFD-induced alterations in the frequency of HSPC populations and the composition of blood cells, despite being divergent between males and females, were both dependent on adipose SCF, underscoring the fundamental niche function of MAT.

Similar to obesity, aging is also associated with increased HSC numbers but decreased regenerative potential and skewed differentiation toward myeloid cells.[54,68,69] Both cell-intrinsic and cell-extrinsic mechanisms are accountable to these aged-related changes. MAT substantially expand in aged humans and rodents, and has been proposed as a suppressor of hematopoiesis in aging.[70] However, in this study, by deleting SCF from adipose tissues, we were able to show that adipose-derived SCF is essential for the expansion of LSK stem cells and all myeloid precursor populations in middle-aged mice. It again supports the notion that MAT provides niche factors for the HSPC, particularly the myeloid compartment. Nevertheless, it is unclear whether such requirement of adipose SCF prevents hematopoietic aging or accelerates the exhaustion of HSPC in the bone marrow. Functional characterization of these HSPC in aged *Adipoq-Cre$^+$;Kitl$^{fl/fl}$* mice is required in future experiments.

In summary, we demonstrate that MAT is a functionally important source of SCF in steady-state hematopoiesis and required for HSPC to cope with metabolic stresses in obesity and aging.

Acknowledgments

We thank Dr. Alessandro Bartolomucci, Dr. Maria Razzoli, and Dr. Pilar Ariza Guzman at the Integrative Biology and Physiology Core for EchoMRI analyses and animal housing in temperature-controlled rooms.

Funding

This work was supported by National Key R&D Program of China (2017YFD0500505), Fundamental Research Funds for the Central Universities (KJQN201604), National Natural and Science Foundation of China (31500944), Natural Science Foundation of Jiangsu Province (BK20150687), and China Scholarship Council postdoctoral fellowship (201606855010) to ZH; Natural Science Foundation of Jiangsu Province (BK20170147) to ZZ; National Natural and Science Foundation of China (81770543), American Diabetes Association (18-IBS-167), and NIAID (R01AId139420 and R21AI140109) to H-BR.

References

1. Brestoff JR, Artis D. Immune regulation of metabolic homeostasis in health and disease. Cell. 2015;161(1):146-160.
2. de Haan G, Lazare SS. Aging of hematopoietic stem cells. Blood. 2018;131(5):479-487.
3. Kovtonyuk LV, Fritsch K, Feng X, Manz MG, Takizawa H. Inflamm-Aging of Hematopoiesis, Hematopoietic Stem Cells, and the Bone Marrow Microenvironment. Front Immunol. 2016;7:502.
4. Despars G, St-Pierre Y. Bidirectional interactions between bone metabolism and hematopoiesis. Exp Hematol. 2011; 39(8):809-816.
5. Kohli L, Passegue E. Surviving change: the metabolic journey of hematopoietic stem cells. Trends Cell Biol. 2014;24(8):479-487.
6. Karigane D, Takubo K. Metabolic regulation of hematopoietic and leukemic stem/progenitor cells under homeostatic and stress conditions. Int J Hematol. 2017;106(1):18-26.
7. Buck MD, Sowell RT, Kaech SM, Pearce EL. Metabolic Instruction of Immunity. Cell. 2017;169(4):570-586.
8. Ganeshan K, Chawla A. Metabolic regulation of immune responses. Annu Rev Immunol. 2014;32:609-634.
9. Trottier MD, Naaz A, Li Y, Fraker PJ. Enhancement of hematopoiesis and lymphopoiesis in diet-induced obese mice. Proc Natl Acad Sci U S A. 2012; 109(20):7622-7629.
10. Singer K, DelProposto J, Morris DL, et al. Diet-induced obesity promotes myelopoiesis in hematopoietic stem cells. Mol Metab. 2014;3(6):664-675.
11. van den Berg SM, Seijkens TT, Kusters PJ, et al. Diet-induced obesity in mice diminishes hematopoietic stem and progenitor cells in the bone marrow. FASEB J. 2016;30(5):1779-1788.
12. Luo Y, Chen GL, Hannemann N, et al. Microbiota from Obese Mice Regulate Hematopoietic Stem Cell Differentiation by Altering the Bone Niche. Cell Metab. 2015;22(5):886-894.
13. Lee JM, Govindarajah V, Goddard B, et al. Obesity alters the long-term fitness of the hematopoietic stem cell compartment through modulation of Gfi1 expression. J Exp Med. 2018;215(2):627-644.
14. Adler BJ, Kaushansky K, Rubin CT. Obesity-driven disruption of haematopoiesis and the bone marrow niche. Nat Rev Endocrinol. 2014; 10(12):737-748.
15. Claycombe K, King LE, Fraker PJ. A role for leptin in sustaining lymphopoiesis and myelopoiesis. Proc Natl Acad Sci U S A. 2008;105(6):2017-2021.
16. Nagareddy PR, Kraakman M, Masters SL, et al. Adipose tissue macrophages promote myelopoiesis and monocytosis in obesity. Cell Metab. 2014;19(5):821-835.
17. Wei Q, Frenette PS. Niches for Hematopoietic Stem Cells and Their Progeny. Immunity. 2018;48(4):632-648.
18. Calvi LM, Link DC. The hematopoietic stem cell niche in homeostasis and disease. Blood. 2015;126(22):2443-2451.
19. Morrison SJ, Scadden DT. The bone marrow niche for haematopoietic stem cells. Nature. 2014;505(7483):327-334.
20. Asada N, Kunisaki Y, Pierce H, et al. Differential cytokine contributions of perivascular haematopoietic stem cell niches. Nat Cell Biol. 2017;19(3):214-223.
21. Greenbaum A, Hsu YM, Day RB, et al. CXCL12 in early mesenchymal progenitors is required for haematopoietic stem-cell maintenance. Nature. 2013;495(7440):227-230.
22. Ding L, Saunders TL, Enikolopov G, Morrison SJ. Endothelial and perivascular cells maintain haematopoietic stem cells. Nature. 2012;481(7382):457-462.
23. Hanoun M, Maryanovich M, Arnal-Estape A, Frenette PS. Neural regulation of hematopoiesis, inflammation, and cancer. Neuron. 2015;86(2):360-373.
24. Mizoguchi T, Pinho S, Ahmed J, et al. Osterix marks distinct waves of primitive and definitive stromal progenitors during bone marrow development. Dev Cell. 2014;29(3):340-349.
25. Liu Y, Strecker S, Wang L, et al. Osterix-cre labeled progenitor cells contribute to the formation and maintenance of the bone marrow stroma. PLoS One. 2013; 8(8):e71318.
26. Chen J, Shi Y, Regan J, Karuppaiah K, Ornitz DM, Long F. Osx-Cre targets multiple cell types besides osteoblast lineage in postnatal mice. PLoS One. 2014; 9(1):e85161.
27. Scheller EL, Cawthorn WP, Burr AA, Horowitz MC, MacDougald OA. Marrow Adipose Tissue: Trimming the Fat. Trends Endocrinol Metab. 2016;27(6):392-403.
28. Suchacki KJ, Cawthorn WP, Rosen CJ. Bone marrow adipose tissue: formation, function and regulation. Curr Opin Pharmacol. 2016;28:50-56.
29. de Paula FJA, Rosen CJ. Structure and Function of Bone Marrow Adipocytes. Compr Physiol. 2017;8(1):315-349.
30. Li Z, Hardij J, Bagchi DP, Scheller EL, MacDougald OA. Development, regulation, metabolism and function of bone marrow adipose tissues. Bone. 2018;110:134-140.
31. Naveiras O, Nardi V, Wenzel PL, Hauschka PV, Fahey F, Daley GQ. Bone-marrow adipocytes as negative regulators of the haematopoietic microenvironment. Nature. 2009;460(7252):259-263.
32. Zhou BO, Yu H, Yue R, et al. Bone marrow adipocytes promote the regeneration of stem cells and haematopoiesis by secreting SCF. Nat Cell Biol. 2017;19(8):891-903.
33. Boyd AL, Reid JC, Salci KR, et al. Acute myeloid leukaemia disrupts endogenous myelo-erythropoiesis by compromising the adipocyte bone marrow niche. Nat Cell Biol. 2017;19(11):1336-1347.
34. Lennartsson J, Ronnstrand L. Stem cell factor receptor/c-Kit: from basic science to clinical implications. Physiol Rev. 2012;92(4):1619-1649.
35. Huang Z, Ruan HB, Zhang ZD, et al. Mutation in the first Ig-like domain of Kit leads to JAK2 activation and myeloproliferation in mice. Am J Pathol. 2014; 184(1):122-132.
36. Ruan HB, Zhang N, Gao X. Identification of a novel point mutation of mouse protooncogene c-kit through N-ethyl-N-nitrosourea mutagenesis. Genetics. 2005; 169(2):819-831.
37. Nishio M, Yoneshiro T, Nakahara M, et al. Production of functional classical brown adipocytes from human pluripotent stem cells using specific hemopoietin cocktail without gene transfer. Cell Metab. 2012; 16(3):394-406.
38. Huang Z, Ruan HB, Xian L, et al. The stem cell factor/Kit signalling pathway regulates mitochondrial function and energy expenditure. Nat Commun. 2014;5:4282.
39. Herault A, Binnewies M, Leong S, et al. Myeloid progenitor cluster formation drives emergency and leukaemic myelopoiesis. Nature. 2017;544(7648):53-58.
40. Fan Y, Hanai JI, Le PT, et al. Parathyroid Hormone Directs Bone Marrow Mesenchymal Cell Fate. Cell Metab. 2017;25(3):661-672.
41. Ambrosi TH, Scialdone A, Graja A, et al. Adipocyte Accumulation in the Bone Marrow during Obesity and Aging Impairs Stem Cell-Based Hematopoietic and Bone Regeneration. Cell Stem Cell. 2017;20(6):771-784 e776.
42. Inra CN, Zhou BO, Acar M, et al. A perisinusoidal niche for extramedullary haematopoiesis in the spleen. Nature. 2015;527(7579):466-471.
43. Broudy VC. Stem cell factor and hematopoiesis. Blood. 1997;90(4):1345-1364.
44. Singer K, Maley N, Mergian T, et al. Differences in Hematopoietic Stem Cells Contribute to Sexually Dimorphic Inflammatory Responses to High Fat Diet-induced Obesity. J Biol Chem. 2015; 290(21):13250-13262.
45. Nakada D, Oguro H, Levi BP, et al. Oestrogen increases haematopoietic stem-cell self-renewal in females and during pregnancy. Nature. 2014;505(7484):555-558.
46. del Toro R, Mendez-Ferrer S. Autonomic regulation of hematopoiesis and cancer. Haematologica. 2013;98(11):1663-1666.
47. Mendez-Ferrer S, Lucas D, Battista M, Frenette PS. Haematopoietic stem cell release is regulated by circadian oscillations. Nature. 2008;452(7186):442-447.
48. Mendez-Ferrer S, Battista M, Frenette PS. Cooperation of beta(2)- and beta(3)-adrenergic receptors in hematopoietic progenitor cell mobilization. Ann N Y Acad Sci. 2010;1192:139-144.
49. Arranz L, Sanchez-Aguilera A, Martin-Perez D, et al. Neuropathy of haematopoietic stem cell niche is essential for myeloproliferative neoplasms. Nature. 2014; 512(7512):78-81.
50. Drexler B, Passweg JR, Tzankov A, et al. The sympathomimetic agonist mirabegron did not lower JAK2-V617F allele burden, but restored nestin-positive cells and reduced reticulin fibrosis in patients with myeloproliferative neoplasms: results of phase 2 study SAKK 33/14. Haematologica. 2019;104(4):710-716.
51. Scheller EL, Khandaker S, Learman BS, et al. Bone marrow adipocytes resist lipolysis and remodeling in response to beta-adrenergic stimulation. Bone. 2019;118:32-41.
52. Scheller EL, Doucette CR, Learman BS, et al. Region-specific variation in the properties of skeletal adipocytes reveals regulated and constitutive marrow adipose tissues. Nat Commun. 2015;6:7808.
53. Povinelli BJ, Kokolus KM, Eng JW, et al. Standard sub-thermoneutral caging temperature influences radiosensitivity of hematopoietic stem and progenitor cells. PLoS One. 2015;10(3):e0120078.
54. Geiger H, de Haan G, Florian MC. The ageing haematopoietic stem cell compartment. Nat Rev Immunol. 2013;13(5):376-389.
55. Wang L, Di L, Noguchi CT. Erythropoietin, a novel versatile player regulating energy metabolism beyond the erythroid system. Int J Biol Sci. 2014;10(8):921-939.
56. Hunt AN, Malur A, Monfort T, et al.

Hepatic Steatosis Accompanies Pulmonary Alveolar Proteinosis. Am J Respir Cell Mol Biol. 2017;57(4):448-458.
57. Tsao CH, Shiau MY, Chuang PH, Chang YH, Hwang J. Interleukin-4 regulates lipid metabolism by inhibiting adipogenesis and promoting lipolysis. J Lipid Res. 2014; 55(3):385-397.
58. Ricardo-Gonzalez RR, Red Eagle A, Odegaard JI, et al. IL-4/STAT6 immune axis regulates peripheral nutrient metabolism and insulin sensitivity. Proc Natl Acad Sci U S A. 2010;107(52):22617-22622.
59. Comazzetto S, Murphy MM, Berto S, Jeffery E, Zhao Z, Morrison SJ. Restricted Hematopoietic Progenitors and Erythropoiesis Require SCF from Leptin Receptor+ Niche Cells in the Bone Marrow. Cell Stem Cell. 2019;24(3):477-486
60. Omatsu Y, Sugiyama T, Kohara H, et al. The essential functions of adipo-osteogenic progenitors as the hematopoietic stem and progenitor cell niche. Immunity. 2010; 33(3):387-399.
61. Mendez-Ferrer S, Michurina TV, Ferraro F, et al. Mesenchymal and haematopoietic stem cells form a unique bone marrow niche. Nature. 2010;466(7308):829-834.
62. Zhou BO, Yue R, Murphy MM, Peyer JG, Morrison SJ. Leptin-receptor-expressing mesenchymal stromal cells represent the main source of bone formed by adult bone marrow. Cell Stem Cell. 2014;15(2):154-168.
63. Zhao M, Tao F, Venkatraman A, et al. N-Cadherin-Expressing Bone and Marrow Stromal Progenitor Cells Maintain Reserve Hematopoietic Stem Cells. Cell Rep. 2019;26(3):652-669 e656.
64. Gao X, Xu C, Asada N, Frenette PS. The hematopoietic stem cell niche: from embryo to adult. Development. 2018;145(2):dev139691
65. Crane GM, Jeffery E, Morrison SJ. Adult haematopoietic stem cell niches. Nat Rev Immunol. 2017;17(9):573-590.
66. Ding L, Morrison SJ. Haematopoietic stem cells and early lymphoid progenitors occupy distinct bone marrow niches. Nature. 2013;495(7440):231-235.
67. Yu VW, Saez B, Cook C, et al. Specific bone cells produce DLL4 to generate thymus-seeding progenitors from bone marrow. J Exp Med. 2015;212(5):759-774.
68. Young K, Borikar S, Bell R, Kuffler L, Philip V, Trowbridge JJ. Progressive alterations in multipotent hematopoietic progenitors underlie lymphoid cell loss in aging. J Exp Med. 2016;213(11):2259-2267.
69. Rossi DJ, Bryder D, Zahn JM, et al. Cell intrinsic alterations underlie hematopoietic stem cell aging. Proc Natl Acad Sci U S A. 2005;102(26):9194-9199.
70. Veldhuis-Vlug AG, Rosen CJ. Clinical implications of bone marrow adiposity. J Intern Med. 2018;283(2):121-139.